Split-Field and Anisotropic-Medium PML–FDTD Implementations for Inhomogeneous Media

Fernando L. Teixeira, *Member, IEEE*, Christopher D. Moss, Weng C. Chew, *Fellow, IEEE*, and Jin A. Kong, *Fellow, IEEE*

***Abstract*—In this paper, we present three-dimensional finite-difference time-domain (FDTD) algorithms for transient simulation of electromagnetic-wave propagation in arbitrary inhomogeneous media, which incorporate the perfectly matched layer (PML) absorbing boundary condition. We discuss the choice of constitutive parameters inside the PML layers to match the interior inhomogeneous media for planar interfaces and corner regions. We illustrate the method using both a split-field PML–FDTD formulation in Cartesian coordinates and an anisotropic medium (unsplit) PML–FDTD formulation in cylindrical coordinates.**

***Index Terms*—Absorbing boundary condition, finite-difference time domain, inhomogeneous media, perfectly matched layer.**

I. Introduction

TIME-DOMAIN simulation of electromagnetic (EM)-wave propagation and scattering in inhomogeneous media is important for a wide range of applications. Analysis of multilayered microstrip antennas and circuits, EM-wave interaction with biological media, and subsurface sensing problems are examples of applications where the host medium is inhomogeneous [1]–[3]. Due to its flexibility in dealing with arbitrary inhomogeneous media, the finite-difference time-domain (FDTD) method has become quite popular for time-domain simulations in those cases [1], [2]. An important issue for the FDTD algorithm in unbounded domain simulations is the truncation of the finite computational domain. Absorbing boundary conditions (ABCs) need to be constructed at the outer boundaries to eliminate spurious reflections from the grid terminations.

In this paper, we discuss the application of the perfectly matched layer (PML) ABC [4] for Cartesian and cylindrical grid three-dimensional (3-D) FDTD simulations in arbitrary inhomogeneous media. We describe the choice of PML parameters to match the inhomogeneous interior media for single interface and corner regions at the outer boundaries of 3-D FDTD domains. We implement the 3-D PML–FDTD schemes through both a split-field PML–FDTD formulation and an unsplit-field (anisotropic-medium) PML–FDTD formulation [5].

Manuscript received May 21, 2000. This work was supported in part by the Air Force Office of Scientific Research Multidisciplinary University Research Initiative under Grant F49620-96-1-0025, by the National Science Foundation under Grant ECS96-15799, and by the Office of Naval Research under Grant N00014-J-92-4098 and Grant N00014-97-1-0172.

F. L. Teixeira was with the Research Laboratory of Electronics, Massachusetts Institute of Technology, Cambridge, MA 02139-4307 USA. He is now with the Department of Electrical Engineering and ElectroScience Laboratory, The Ohio State University, Columbus, OH 43212-1191 USA (e-mail: teixeira@ee.eng.ohio-state.edu).

C. D. Moss and J. A. Kong are with the Research Laboratory of Electronics, Department of Electrical Engineering and Computer Science, Massachusetts Institute of Technology, Cambridge, MA 02139-4307 USA (e-mail: cmoss@mit.edu).

W. C. Chew is with the Center for Computational Electromagnetics, Electromagnetics Laboratory, Department of Electrical and Computer Engineering, University of Illinois at Urbana-Champaign, Urbana, IL 61801-2991 USA.

Publisher Item Identifier S 0018-9480(02)00748-2.

II. Split-Field Formulation in Cartesian Coordinates for Inhomogeneous Media

In the split-field PML formulation [4]–[7], EM fields components are split into subcomponents and matched artificial (electric and magnetic) conductivities are introduced inside the PML. The split-field approach was shown to be equivalent to an analytic continuation (continuous mapping) of Maxwell's equations to a complex spatial domain (complex space) [6], [7]. The advantage of recognizing the PML as an analytic continuation is that the PML implementation becomes *transparent* to the particular constitutive properties of the medium. This should be expected since the PML is a (material) local boundary condition, and its implementation should depend only on the *local* material properties of the medium. In order to match an interior homogeneous media with μ and ϵ, the constitutive parameters of the PML are set equal to those in the interior domain. The PML region is then set up as the region where the analytic continuation of the spatial coordinates is enforced [6], [7].

In arbitrary inhomogeneous media, Maxwell's equations are written as

$$\nabla \times \mathbf{H} = -i\omega\epsilon(\mathbf{r})\mathbf{E} + \sigma(\mathbf{r})\mathbf{E} \tag{1a}$$

$$\nabla \times \mathbf{E} = i\omega\mu(\mathbf{r})\mathbf{H}. \tag{1b}$$

The PML is defined through the analytic continuation on the spatial variables, i.e., by a continuous mapping of the spatial variables x, y, and z into complex variables $\tilde{x}$, $\tilde{y}$, and $\tilde{z}$ through ($e^{-i\omega t}$ convention) [6], [7]

$$\zeta \rightarrow \tilde{\zeta} = \int_0^{\zeta} s_\zeta(\zeta')d\zeta' = b_\zeta(\zeta) + i\frac{\Delta_\zeta(\zeta)}{\omega} \tag{2}$$

with

$$s_\zeta(\zeta) = a_\zeta(\zeta) + i\frac{\Omega_\zeta(\zeta)}{\omega} \tag{3}$$

with $\zeta = x, y, z$.

As a result, the modified nabla operator for Cartesian coordinates inside the PML is given by [6]

$$\tilde{\nabla} = \hat{x}\frac{\partial}{\partial\tilde{x}} + \hat{y}\frac{\partial}{\partial\tilde{y}} + \hat{z}\frac{\partial}{\partial\tilde{z}} = \hat{x}\frac{1}{s_x}\frac{\partial}{\partial x} + \hat{y}\frac{1}{s_y}\frac{\partial}{\partial y} + \hat{z}\frac{1}{s_z}\frac{\partial}{\partial z}. \tag{4}$$

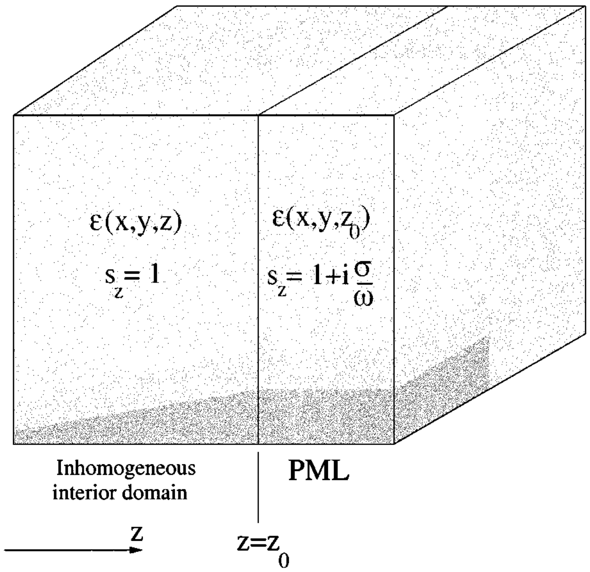

Fig. 1. Reflectionless PML interface can be designed by inheriting the interior constitutive parameters at the interface and through enforcement of the analytic continuation of spatial coordinates.

Upon substituting (4) into (1), modified Maxwell's equations result inside the PML, i.e.,

$$\tilde{\nabla} \times \mathbf{H} = -i\omega\epsilon(\mathbf{r})\mathbf{E} + \sigma(\mathbf{r})\mathbf{E} \tag{5a}$$

$$\tilde{\nabla} \times \mathbf{E} = i\omega\mu(\mathbf{r})\mathbf{H} \tag{5b}$$

where $\epsilon(\mathbf{r})$, $\mu(\mathbf{r})$, and $\sigma(\mathbf{r})$ in (5) are the same as those in (1) so that continuity is preserved across the physical-domain-to-PML interface.

To minimize reflections, the constitutive parameters $\epsilon(\mathbf{r})$ and $\mu(\mathbf{r})$ at any transverse plane inside the PML are equal to those at the physical-domain-to-PML interface, and invariant along the *normal* direction to the interface. This is illustrated in Fig. 1 for a planar PML along the z-direction. Note that potential inhomogeneities present in the *transverse* directions will eventually produce reflections inside the PML. However, such reflections contribute only along the transverse directions, as illustrated in Fig. 2 (for a continuously inhomogeneous media, those will be distributed reflections). This PML construction for inhomogeneous media preserves the two important characteristics of a PML layer, i.e.: 1) zero reflection coefficients (in the continuum limit) at the PML interface and 2) exponential decay along the normal direction.

By taking (5) on an inhomogeneous media with conductive loss, splitting the fields (i.e., $\mathbf{E} = \mathbf{E}_{sx} + \mathbf{E}_{sy} + \mathbf{E}_{sz}$, with $\mathbf{E}_{sx} = \mathbf{y}E_{sxy} + \mathbf{z}E_{sxz}$, etc.), and transforming back to time domain, the following equations are obtained for the $\mathbf{E}_{s\zeta}$ and $\mathbf{H}_{s\zeta}$ subcomponents

$$a_\zeta \frac{\partial}{\partial t}\mu(\mathbf{r})\mathbf{H}_{s\zeta} + \Omega_\zeta\mu(\mathbf{r})\mathbf{H}_{s\zeta} = -\hat{\zeta} \times \frac{\partial}{\partial \zeta}\mathbf{E} \tag{6}$$

$$a_\zeta\epsilon(\mathbf{r})\frac{\partial}{\partial t}\mathbf{E}_{s\zeta} + \Omega_\zeta\epsilon(\mathbf{r})\mathbf{E}_{s\zeta} + a_\zeta\sigma(\mathbf{r})\mathbf{E}_{s\zeta}\Omega_\zeta\sigma(\mathbf{r})\int_0^t \mathbf{E}_{s\zeta}(\tau)\,d\tau = \hat{\zeta} \times \frac{\partial}{\partial \zeta}\mathbf{H}. \tag{7}$$

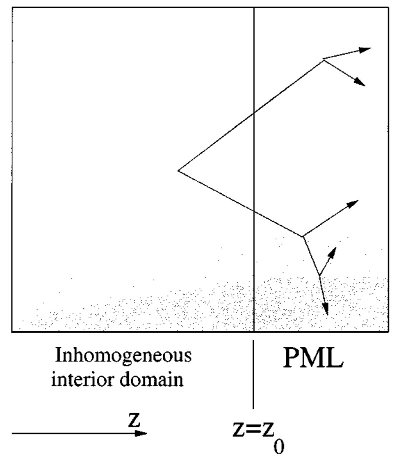

Fig. 2. Ray picture of the reflection mechanism inside the PML matched to an inhomogeneous medium.

From (6) and (7), the update for the magnetic field is given by

$$\mathbf{H}_{s\zeta}^{l+(1/2)} = -(a_\zeta + \Omega_\zeta\Delta_t)^{-1} \cdot \left[\frac{1}{\mu(\mathbf{r})}\Delta_t\left(\hat{\zeta} \times \frac{\partial}{\partial\zeta}\mathbf{E}^l\right) - a_\zeta\mathbf{H}_{s\zeta}^{l-(1/2)}\right] \tag{8}$$

and the update equations for the electric field is given by

$$\mathbf{E}_{s\zeta}^{l+1} = \Big[(a_\zeta + \Omega_\zeta\Delta_t)\,\epsilon(\mathbf{r}) + a_\zeta\sigma(\mathbf{r})\Delta_t\Big]^{-1} \cdot \Bigg[\Delta_t\left(\hat{\zeta} \times \frac{\partial}{\partial\zeta}\mathbf{H}^{l+(1/2)}\right) + a_\zeta\epsilon(\mathbf{r})\mathbf{E}_{s\zeta}^l - \sigma(\mathbf{r})\Omega_\zeta\Delta_t\mathbf{F}_{s\zeta}^l\Bigg] \tag{9}$$

with

$$\mathbf{F}_{s\zeta}^l = \mathbf{F}_{s\zeta}^{l-1} + \frac{1}{2}\left(\mathbf{E}_{s\zeta}^l + \mathbf{E}_{s\zeta}^{l-1}\right)\Delta_t. \tag{10}$$

Similar split-field schemes can be derived in other coordinate systems [7].

For the corner regions, the values of $\epsilon(\mathbf{r})$, $\mu(\mathbf{r})$, and $\sigma(\mathbf{r})$ inside the PML are taken from the interior-to-PML *line* (instead of plane) interface in case of a edge corner or from the interior-to-PML *point* interface in case of a vertex corner (3-D geometry).

An important observation is in order. The objective of the PML construction in inhomogeneous media described here is to produce a reflectionless interface and to eliminate the spurious reflections from the grid terminations. However, the resulting solution obtained in the finite PML–FDTD domain may not, for some inhomogeneous problems, correspond to the actual solution (unbounded domain) in mind. This is because the PML is designed to suppress *all* reflections from the outer domain while, for some inhomogeneous media problems (e.g., unbounded random media or rough surfaces), some amount of reflection from the outer region is nevertheless present. For those problems, however, the truncation error is of a different nature [8], [9] (and is present even in integral-equation-based methods [9]). Mathematically, this is expressed by the fact that a Sommerfeld-like radiation condition cannot be invoked in such cases. For many inhomogeneous problems of practical interest however (e.g., layered media problems), the truncated

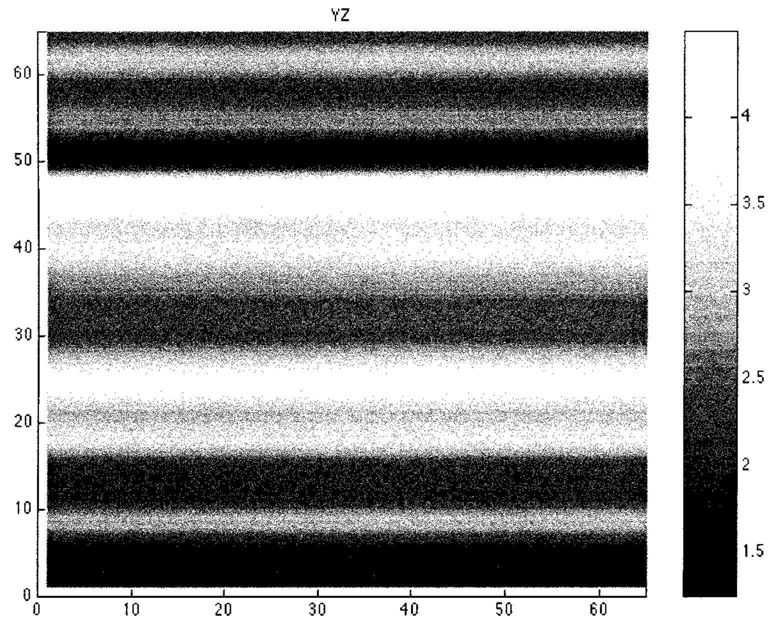

Fig. 3. Permittivity profile of a stratified random medium with Gaussian correlation function in the z-direction.

PML–FDTD solution and the infinite-domain solution do coincide.

III. Anisotropic-Medium Formulation in Cylindrical Coordinates for Inhomogeneous Media

The unsplit field formulation of the PML is an alternative formulation where the spatial operators in the Maxwell's equations retain their usual form and the constitutive relations are modified. The resultant fields inside the PML can be associated with those of an anisotropic medium with particular electric and magnetic constitutive tensors.

To illustrate the generality of the approach, here we will consider 3-D cylindrical coordinates instead of Cartesian coordinates. In the case of 3-D cylindrical coordinates, the PML constitutive tensors matched to a homogeneous medium, characterized by constitutive parameters ϵ and μ, are written as [7], [10]

$$\bar{\bar{\epsilon}}_{\rm PML} = \epsilon\bar{\bar{\Lambda}}_{[\rho,\phi,z]}(\rho, z;\omega) \tag{11a}$$

and

$$\bar{\bar{\mu}}_{\rm PML} = \mu\bar{\bar{\Lambda}}_{[\rho,\phi,z]}(\rho, z;\omega) \tag{11b}$$

where

$$\bar{\bar{\Lambda}}_{[\rho,\phi,z]}(\rho, z;\omega) = \hat{\rho}\hat{\rho}\frac{\tilde{\rho}s_z}{\rho s_\rho} + \hat{\phi}\hat{\phi}\frac{\rho s_z s_\rho}{\tilde{\rho}} + \hat{z}\hat{z}\frac{\tilde{\rho}s_\rho}{\rho s_z}. \tag{12}$$

These constitutive parameters produce a cylindrically layered PML medium matched to the interior medium for all frequencies and angles of incidence.

Since the perfect matching condition is a *local* condition in space, we can apply the condition locally in order to match a inhomogeneous interior medium with $\epsilon(\mathbf{r})$ and $\mu(\mathbf{r})$, i.e.,

$$\bar{\bar{\epsilon}}_{\rm PML} = \epsilon(\mathbf{r})\bar{\bar{\Lambda}}_{[\rho,\phi,z]}(\rho, z;\omega) \tag{13a}$$

$$\bar{\bar{\mu}}_{\rm PML} = \mu(\mathbf{r})\bar{\bar{\Lambda}}_{[\rho,\phi,z]}(\rho, z;\omega). \tag{13b}$$

Inside the PML, the values for $\epsilon(\mathbf{r})$ and $\mu(\mathbf{r})$ in (13) are chosen equal to those at the interior-domain-to-PML interface, as explained in Section II.

Maxwell's equations in a inhomogeneous media with $\epsilon(\mathbf{r})$ and μ are, therefore, written as

$$i\omega\mu\bar{\bar{\Lambda}}_{[\rho,\phi,z]}\cdot\mathbf{H} = \nabla\times\mathbf{E} \tag{14a}$$

$$i\omega\left(1 + i\frac{\sigma(\mathbf{r})}{\omega\epsilon(\mathbf{r})}\right)\epsilon(\mathbf{r})\bar{\bar{\Lambda}}_{[\rho,\phi,z]}\cdot\mathbf{E} = -\nabla\times\mathbf{H} \tag{14b}$$

which may be written, in terms of auxiliary fields $\mathbf{B}_a$, $\mathbf{D}_a$, $\mathbf{E}_a$ simply as

$$i\omega\mu\mathbf{H}_a = \nabla\times\mathbf{E} \tag{15a}$$

$$-i\omega\mathbf{D}_a + \sigma\mathbf{E}_a = \nabla\times\mathbf{H} \tag{15b}$$

where $\mathbf{H}_a = \bar{\bar{\Lambda}}_{[\rho,\phi,z]}\cdot\mathbf{H}$, $\mathbf{D}_a = \bar{\bar{\Lambda}}_{[\rho,\phi,z]}\cdot\mathbf{D}$, and $\mathbf{E}_a = \bar{\bar{\Lambda}}_{[\rho,\phi,z]}\cdot\mathbf{E}$. By comparing these equations with the split-field, it is seen that the update for the auxiliary fields $\mathbf{B}_a$, $\mathbf{D}_a$, and $\mathbf{E}_a$ is just an unsplit version of the split-field update scheme with $s_\zeta = 1$. Therefore, the update of the auxiliary fields in terms of the original ones is just a special case of the update scheme of the Section II. To complete the overall update, we need to update the original fields from the auxiliary ones. To do so, we use the definition of the auxiliary fields directly, which, in the time domain, reduces to a simple system of auxiliary first-order differential equations.

IV. Numerical Results and Analysis

To discuss the implementation of the PML–FDTD algorithm in inhomogeneous media, we consider two distinct scenarios.

First, we simulate a z-directed Hertzian dipole radiating in a layered medium, where the permittivity profile is a particular realization of a random medium with a Gaussian correlation function in the z-direction. The medium is homogeneous in the

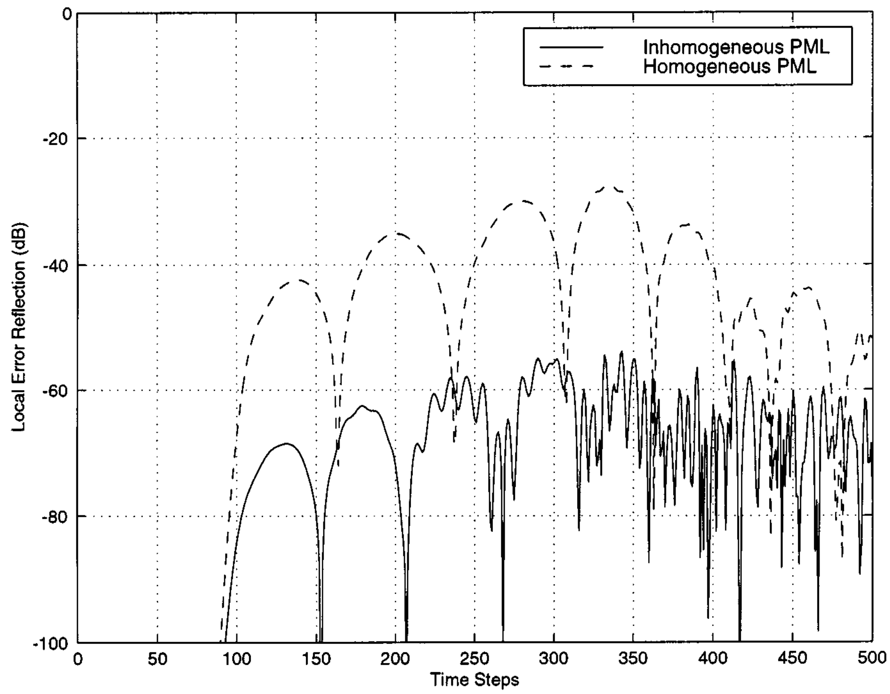

Fig. 4. Local reflection error for the Cartesian PML in the inhomogeneous media of Fig. 3.

x- and y-directions. The particular profile obtained is depicted in Fig. 3. In this example, the theoretical $\langle\epsilon_r\rangle$ is 3, and the actual $\langle\epsilon_r\rangle$ is 2.8. The correlation length is 0.4 m, which comprise 20 grid cells. The variance is 25%. The source is located at the center of the 3-D FDTD domain. The source pulse is a derivative of the Blackman–Harris (BH) pulse with center frequency $f_c = 200$ MHz. We use an eight-layer PML with a quadratic taper. Fig. 4 depicts the local reflection error using the Cartesian PML matched to the interior domain, and implemented as discussed in Section III. The reflection error is compared against an homogeneous PML using $\epsilon_r = 2.8$. The local reflection error is defined as the difference of the electric field PML–FDTD results against those of a much larger benchmark FDTD domain where reflections from the grid terminations are causally isolated. The reflection error is measured two cells away from the PML interface. From Fig. 4, we see that the reflection error using the correct (inhomogeneous on z) PML parameters is order of magnitudes lower than using a homogeneous PML.

Next, we illustrate results for the anisotropic-medium cylindrical PML implementation in a inhomogeneous medium. The 3-D PML–FDTD domain is discretized using a $(N_\rho, N_\phi, N_z) = (20, 40, 50)$ grid. The PML comprises the outer ten cells in the ρ-direction and the top and bottom ten cells in the z-direction, we use a quadratic profile for the PML. We simulate the radiation of a z-oriented electric Hertzian dipole located at $\rho = 0$ and $N_z = 25$ in a medium having $\epsilon_r = \epsilon_c$ and $\sigma = \sigma_c$ for $\rho < 5cm$ and $\epsilon_r = \epsilon_c[1 + \alpha \cos(m\theta)]$ and $\sigma = \sigma_c[1 + \beta \cos(m\theta)]$ for $\rho > 5$ cm. This is a contrived example of an azimuthally inhomogeneous media to demonstrate the method. The source pulse is again a derivative of a BH pulse with center frequency $f_c = 200$ MHz. Fig. 5 depicts the local reflection error using an azimuthally inhomogeneous anisotropic-medium cylindrical PML matched to the interior domain with $\epsilon_c = 2$, $m = 2$, $\sigma = 10^{-6}$, $\alpha = 0.5$, and $\beta = 10$,

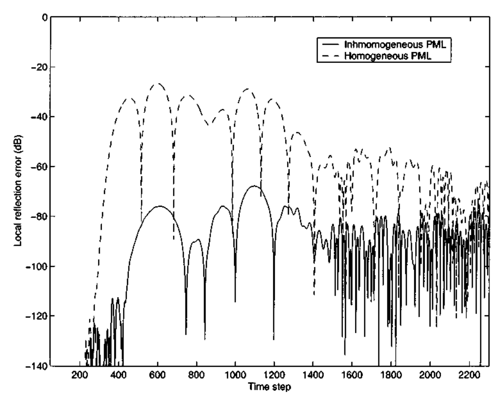

Fig. 5. Local reflection error for the cylindrical PML in inhomogeneous media.

and implemented as discussed in Section III. The reflection error is compared against an anisotropic-medium cylindrical PML with no azimuthal variation at on its constitutive parameters $\epsilon_r = \epsilon_c$ and $\sigma = \sigma_c$. Again, the local reflection error is defined as the difference of the electric field PML–FDTD results against those of a much larger benchmark FDTD domain, and it is measured one cell away from the PML interface. From Fig. 5, we see that, also in this case, the reflection error using the correct inhomogeneous PML parameters is order of magnitudes lower than using a PML with no azimuthal variation. For larger m, we have encountered high-frequency instabilities depending on the size of the FDTD domain (for the domain size above, for $m > 3$). We are currently investigating their origin and best filtering schemes to suppress them. Fig. 6 shows the three snapshots of the squared magnitude of the electric-field evolution on a transversal plane slice of the 3-D grid. The observation plane is three cells away from the source plane in the z-direction. Since the z directed dipole is located

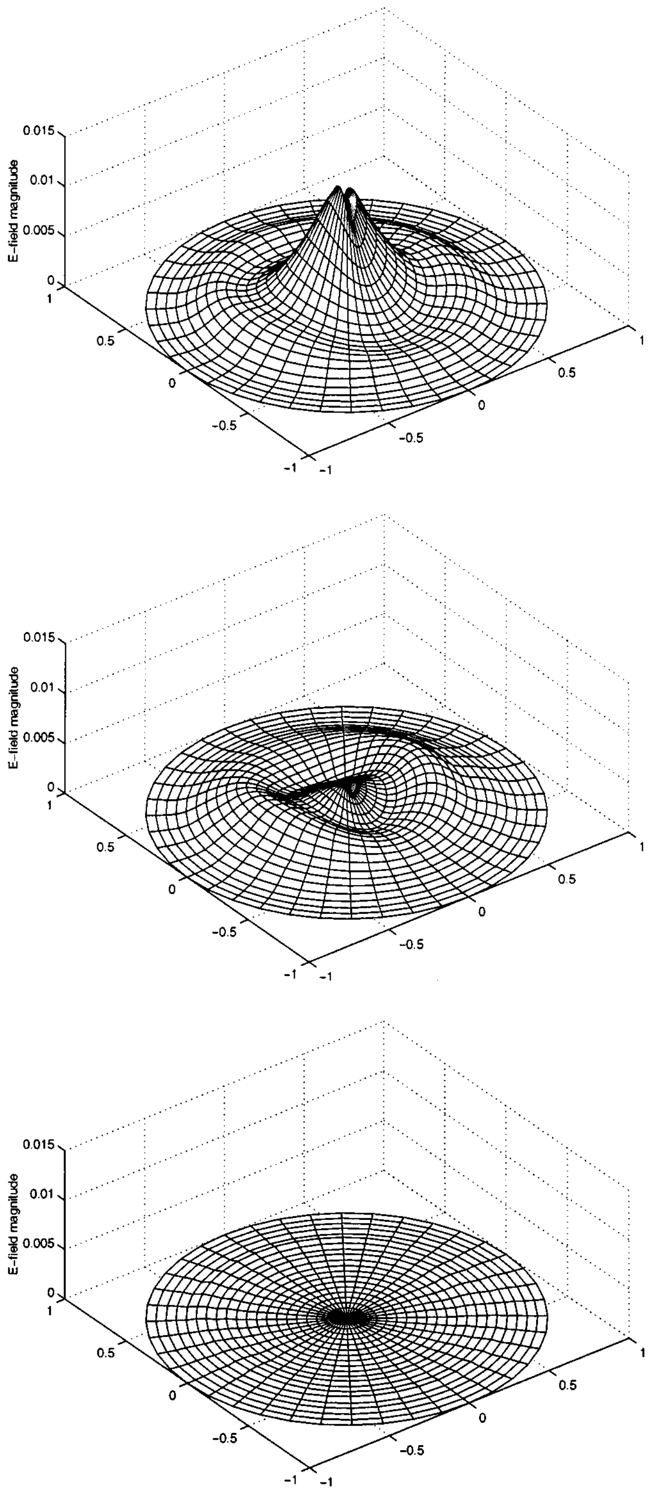

Fig. 6. Snapshots of the electric-field intensity at a horizontal plane of the 3-D cylindrical FDTD domain. The source is z-oriented Hertzian dipole located at the z-axis so that the asymmetry on the field distribution is entirely due to the medium inhomogeneities. The strong attenuation as the wave enters the PML layer is also clearly visible.

at the center of the grid, Fig. 6 serves to illustrate the effect of the medium inhomogeneities on the magnitude profile. The asymmetry present in the profile is entirely due to the inhomogeneities. Moreover, the strong attenuation as the wave enters the PML layer is clearly visible.

V. Conclusions

We discussed the application of PML–FDTD algorithms in inhomogeneous media using both the split-field PML formulation and the anisotropic-medium (unsplit) PML formulation. For the split-field formulation, we described the implementation in Cartesian coordinates, while for the anisotropic-medium formulation, we described the implementation in cylindrical coordinates. It was shown that, by using the interpretation of the PML as a analytic continuation to a complex variables spatial domain, both implementations can be made transparent to the particular constitutive properties of the medium. Numerical examples were given to illustrate the discussion.

References

[1] *Advances in Computational Electrodynamics: The Finite-Difference Time-Domain Method*, A. Taflove, Ed., Artech House, Norwood, MA, 1998.

[2] W. C. Chew, *Waves and Fields in Inhomogeneous Media*. New York: Van Nostrand, 1990.

[3] K. Radhakrishnan and W. C. Chew, "Full-wave analysis of multiconductor transmission lines on anisotropic inhomogeneous substrates," *IEEE Trans. Microwave Theory Tech.*, vol. 47, pp. 1764–1770, Sept. 1999.

[4] J. Berenger, "A perfectly matched layer for the absorption of electromagnetic waves," *J. Comput. Phys.*, vol. 114, no. 2, pp. 185–200, 1994.

[5] S. D. Gedney, "The perfectly matched layer absorbing medium," in *Advances in Computational Electrodynamics: The Finite-Difference Time-Domain Method*, A. Taflove, Ed. Norwood, MA: Artech House, 1998.

[6] F. L. Teixeira and W. C. Chew, "A general approach to extend Berenger's absorbing boundary condition to anisotropic and dispersive media," *IEEE Trans. Antennas Propagat.*, vol. 46, pp. 1386–1387, Sept. 1998.

[7] ——, "Finite-difference simulation of transient electromagnetic fields for cylindrical geometries in complex media," *IEEE Trans. Geosci. Remote Sensing*, vol. 38, pp. 1530–1543, July 2000.

[8] F. D. Hastings and J. B. Schneider, "A Monte Carlo FDTD technique for rough surface scattering," *IEEE Trans. Antennas Propagat.*, vol. 43, pp. 1183–1191, Nov. 1995.

[9] J. T. Johnson, R. T. Shin, J. A. Kong, L. Tsang, and K. Pak, "A numerical study of the composite surface model for ocean backscattering," *IEEE Trans. Geosci. Remote Sensing*, vol. 36, pp. 72–83, Jan. 1998.

[10] F. L. Teixeira and W. C. Chew, "Systematic derivation of anisotropic PML absorbing media in cylindrical and spherical coordinates," *IEEE Microwave Guided Wave Lett.*, vol. 7, pp. 371–373, Nov. 1997.

Fernando L. Teixeira (S'89–M'93) received the B.S. and M.S. degrees from the Pontifical Catholic University of Rio de Janeiro, Rio de Janeiro, Brazil, in 1991 and 1995, respectively, and the Ph.D. from the University of Illinois at Urbana-Champaign, Urbana, in 1999, all in electrical engineering.

From 1994 to 1996, he was with the Satellite Transmission Department, EMBRATEL S.A. (MCI/WorldCom), Rio de Janeiro, Brazil. From 1996 to 1999, he was a Research Assistant with the University of Illinois at Urbana-Champaign. From 1999 to 2000, he was a Post-Doctoral Associate at the Massachusetts Institute of Technology (MIT), Cambridge. Since 2000, he has been and Assistant Professor with the Department of Electrical Engineering and ElectroScience Laboratory (ESL), The Ohio State University, Columbus, OH. His current research interests include wave-propagation modeling for communication, sensing, and device applications. He has authored or co-authored over 20 journal papers.

Dr. Teixeira is a member of Phi Kappa Phi. He was the Technical Program coordinator of PIERS 2000, Cambridge, MA. He was a recipient of the 1998 IEEE Microwave Theory and Techniques Society (IEEE MTT-S) Fellowship Award, the 1999 Raj Mittra Outstanding Research Award presented by the University of Illinois at Urbana-Champaign, and paper awards presented at the 1999 USNC/URSI Meeting (Boulder, CO) and the 1999 IEEE Antennas and Propagation Society (IEEE AP-S) International Symposium (Orlando, FL).

Christopher D. Moss received the B.S. degree from the University of Alberta, Edmonton, AB, Canada, in 1996, the M.S. degree from the Massachusetts Institute of Technology (MIT), Cambridge, in 2000, both in electrical engineering, and is currently working toward the Ph.D. degree in electrical engineering at MIT.

From 1997 to 1998, he was an Engineer in the Microwave Systems Department, Raytheon, where he was mainly involved in monolithic-microwave integrated-circuit (MMIC) design. Since 1998, he has been a Research Assistant with the Center for Electromagnetic Theory and Applications, MIT. His research interests include both analytical and computational methods in electromagnetics for remote sensing and communication applications.

Weng C. Chew (S'79–M'80–SM'86–F'93) received the B.S., M.S. and Engineer's, and Ph.D. degrees from the Massachusetts Institute of Technology (MIT), Cambridge, in 1976, 1978, and 1980, all in electrical engineering.

From 1981 to 1985, he was with Schlumberger-Doll Research, Ridgefield, CT, where, he was a Program Leader and later a Department Manager. From 1985 to 1990, he was an Associate Professor with the Department of Electrical and Computer Engineering, University of Illinois at Urbana-Champaign. He currently is a Professor at the University of Illinois at Urbana-Champaign. From 1989 to 1993, he was the Associate Director the Advanced Construction Technology Center, University of Illinois at Urbana-Champaign. He is currently the Director of the Center for Computational Electromagnetics and the Electromagnetics Laboratory, University of Illinois at Urbana-Champaign, and also holds a Distinguished Founder Professorship. He authored *Waves and Fields in Inhomogeneous Media* (Piscataway, NJ: IEEE Press, 1995), authored or co-authored over 200 scientific journal articles, and presented over 270 conference papers. He is listed in the University of Illinois at Urbana-Champaign's *List of Excellent Instructors*. He is an Associate Editor for the *Journal of Electromagnetic Waves and Applications* (1996–present), and *Microwave Optical Technology Letters* (1996–present). His recent research interest include wave propagation, scattering, inverse scattering, and fast algorithms related to scattering.

Dr. Chew is a member of Eta Kappa Nu, Tau Beta Pi, and URSI Commissions B and F. He was also an AdCom member of the IEEE Geoscience and Remote Sensing Society, and is currently an associate editor of the IEEE TRANSACTIONS ON GEOSCIENCE AND REMOTE SENSING (1984–present). He was the recipient of the 2000 IEEE Graduate Teaching Award and was a 1986 National Science Foundation (NSF) Presidential Young Investigator.

Jin A. Kong (S'65–M'69–SM'74–F'85) is currently a Professor of electrical engineering at the Massachusetts Institute of Technology (MIT), Cambridge, where he is also the Chairman of Area IV on Energy and Electromagnetic Systems, Department of Electrical Engineering and Computer Science, and Director of the Center for Electromagnetic Theory and Applications, Research Laboratory of Electronics. He is the President of The Electromagnetics Academy. He has authored or co-authored over 20 books, including *Electromagnetic Wave Theory* (Cambridge, MA: EMW, 2000), over 200 refereed articles and book chapters, over 300 conference papers, and has supervised over 150 theses. His research interest is in the area of EM-wave theory and applications. He has served as consultant, external examiner, and advisor to industry, academia, national governments, and the United Nations. He is the Editor-in-Chief of the *Journal of Electromagnetic Waves and Applications*, Chief Editor of the PIER book series "Progress in Electromagnetics Research," and Editor of the John Wiley Series in "Remote Sensing."

Dr. Kong is a Fellow of the Optical Society of America (OSA).